RSC Advances

PAPER

View Article Online
View Journal | View Issue

Cite this: *RSC Adv.*, 2017, **7**, 55582

Achieving a high-efficiency dual-core chromophore for emission of blue light by testing different side groups and substitution positions†

Hwangyu Shin,‡[b] Beomjin Kim,‡[a] Hyocheol Jung,[a] Jaehyun Lee,[b] Hayoon Lee,[a] Seokwoo Kang,[a] Jiwon Moon,[b] Joonghan Kim[b] and Jongwook Park*[a]

Hetero dual-core derivatives that combine anthracene and pyrene were systematically studied for the purpose of producing highly efficient blue light-emitting materials applicable to organic light-emitting diode (OLED) lighting. Five compounds were designed in order to (1) determine which one of the two core chromophores in a hetero dual-core moiety, if any, acts as the main contributor to the optical and electronic properties of the final compounds, (2) control the electron-donating ability of the side group, and (3) change the substitution position. 1-[1,1′;3′,1″]terphenyl-5′-yl-6-(10-[1,1′;3′,1″]terphenyl-5′-yl-anthracen-9-yl)-pyrene (**TP-AP-TP**) was used as the reference material, and four other materials, including diphenyl-[10-(6-[1,1′;3′,1″]terphenyl-5′-yl-pyren-1-yl)-anthracen-9-yl]-amine (**DPA-AP-TP**), diphenyl-[6-(10-[1,1′;3′,1″]terphenyl-5′-yl-anthracen-9-yl)-pyren-1-yl]-amine (**TP-AP-DPA**), diphenyl-{4-[10-(6-[1,1′;3′,1″]-terphenyl-5′-yl-pyren-1-yl)-anthracen-9-yl]-phenyl}-amine (**TPA-AP-TP**) and diphenyl-{4-[6-(10-[1,1′;3′,1″]terphenyl-5′-yl-anthracen-9-yl)-pyren-1-yl]-phenyl}-amine (**TP-AP-TPA**), were synthesized as model compounds. The synthesized materials showed absorption wavelength peaks at 403–410 nm in the film state and exhibited PL emissions of 458–505 nm. Also, anthracene was shown to be the main core contributing to the optical and electronic properties. Among the synthesized molecules, the **TPA-AP-TP** molecule, in which triphenylamine, with its optimum electron-donating ability, was substituted into anthracene, showed excellent electroluminescence (EL) performance for OLED lighting with a current efficiency of 8.05 cd A^{-1}, external quantum efficiency of 6.75%, and narrow EL FWHM of 53 nm.

Received 25th October 2017
Accepted 30th November 2017

DOI: 10.1039/c7ra11773f

rsc.li/rsc-advances

1. Introduction

Organic light-emitting diodes (OLEDs) have attracted considerable attention in both academic and industrial circles since the pioneering work of Tang and Vanslyke in 1987. Because of advantageous properties such as self-emission, full-color emission, low driving voltage, flexibility and fast response time, OLEDs have recently been developed and applied extensively in the small and medium display market, and many studies are underway for their applications in television and lighting.[1] Certain properties of OLEDs make them especially attractive in the lighting market, including area emission characteristics not found for other existing sources of light, environmentally friendly efficient use of energy, large area, ultra-light weight, and ultra-thin shape. It has thus become increasingly important to carry out investigations of the applications of OLEDs if they are to become the next-generation source of lighting and replace existing fluorescent and incandescent lamps.[2] White OLEDs for lighting can be divided into those that produce white light by combining red-light, green-light, and blue-light (R, G, B) emitters[3] and those that produce white light by combining emitters of sky-blue light and orange light or of sky-blue light and red light.[4] Investigations have been more actively pursued for the latter two-color white OLEDs whose structures are relatively simple, because low cost is regarded as important in the lighting field, unlike in the display field. In addition, since the emission spectra of organic materials generally have peaks with broader wavelengths than do the emission spectra of inorganic materials, only two types of organic emitters, in particular the emitters of sky-blue and orange light or of sky-blue and red light, need to be combined to produce white light when using OLEDs. Many studies have achieved high efficiency and long lifetime for materials that emit orange or red light, but it has been a challenge to develop materials that emit pure blue light with high efficiency because of the large difference in the energy

[a]*Department of Chemical Engineering, Kyung Hee University, Gyeonggi-do, 17104, Republic of Korea. E-mail: jongpark@khu.ac.kr*

[b]*Department of Chemistry, The Catholic University of Korea, Bucheon, 420-743, Republic of Korea*

† Electronic supplementary information (ESI) available. See DOI: 10.1039/c7ra11773f

‡ These authors contributed equally to this work.

levels of adjacent hole- and electron-transporting layers caused by the wide band gap.[5]

To overcome such issues and increase the efficiency of materials that emit blue light, most existing studies have used polycyclic aromatic hydrocarbon (PAH) moieties based on a single-core chromophore, such as anthracene,[6] pyrene,[7] and fluorene,[8] which have excellent fluorescence characteristics. Studies have been actively conducted, especially with the anthracene core, to increase color purity and electroluminescence (EL) efficiency by adjusting dihedral angles of the core of the molecule or by introducing bulky groups or electron donor and acceptor groups as side groups.[9] Furthermore, the most recent studies have focused on molecules consisting of multi-core chromophore structures by combining two or more of the same PAH core moieties or by combining different such moieties.[10] Our group has recently reported dual-core chromophores of the "AP-core type" where anthracene and pyrene cores were directly connected. These dual-core derivatives showed outstanding performances, with the EL efficiency and device lifetime increased by more than a factor of two compared to light-emitting materials that applied anthracene or pyrene as a single-core chromophore.[11] Unlike the corresponding single-core materials, these dual-core structures displayed high efficiency because both anthracene and pyrene contributed to the absorption and emission processes.[12] However, few studies on such hetero-type dual cores have been published, and there are also few published papers on the roles of core, types of side group and various substitution changes regarding on molecular structure. Accordingly, in order to develop blue light-emitting materials for highly efficient OLED lighting devices, this study examined hetero dual-core moieties in which anthracene and pyrene are connected. We specifically investigated not only which, if any, of the two core chromophores act as the main contributor to the absorption and emission processes, but also the effects of changing the side group on the performance properties of the final compounds. Therefore, (1) a hetero dual-core moiety consisting of anthracene and pyrene (AP-core) was selected as the standard core chromophore; (2) a nitrogen atom was introduced instead of a phenyl ring in order to increase electron donation to the dual core and hence increase device efficiency, (3) a bulky side group was introduced to suppress intermolecular interactions, and (4) the position at which the electron-donating side group is bonded to the dual core was changed to study the effects of changes in the substitution position on the characteristics of the material.

2. Results and discussion

2.1 Molecular design, synthesis, and optical properties

As previously reported by our group, 1-[1,1′;3′,1″]terphenyl-5′-yl-6-(10-[1,1′;3′,1″]terphenyl-5′-yl-anthracen-9-yl)-pyrene (**TP-AP-TP**), which includes anthracene and pyrene as a hetero dual core, yielded a better performance, with about two times higher EQE values and two times longer blue emission lifetimes than their single core counterparts.[11]

Moreover, oscillator strength is closely associated with the electronic transition of the molecule, and an increase of the oscillator strength indicates a contribution of greater energy to the electronic transition at that absorption wavelength. For the AP core, the oscillator strength value of anthracene was

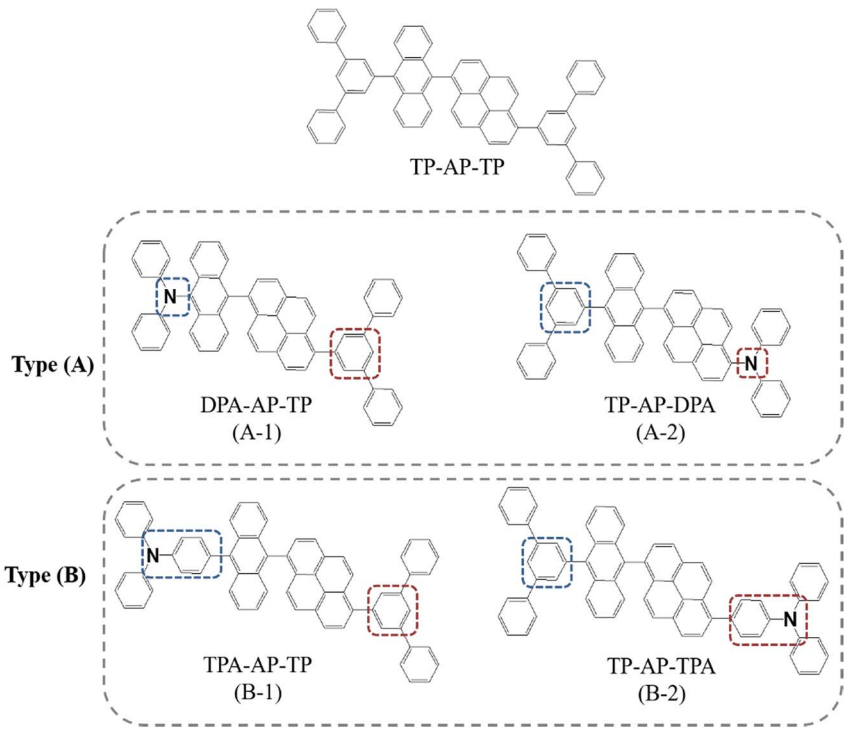

Scheme 1 The chemical structures of the synthesized light-emitting materials based on dual-core chromophores.

Table 1 Optical and thermal properties of the synthesized compounds

Compounds	Solution[a] UV (nm)	PL (nm)	FWHM (nm)	Film[b] UV (nm)	PL (nm)	FWHM (nm)	T_g	T_m	T_d	HOMO (eV)	LUMO (eV)	Band gap (eV)
TP-AP-TP	379, 399	446	56	382, 403	458	53	243	—	480	−6.01	−3.05	2.96
DPA-AP-TP	357, 428	513	65	365, 437	505	59	194	317	497	−5.55	−3.04	2.51
TP-AP-DPA	383, 404	481	67	388, 410	487 502	106	199	—	488	−5.44	−2.76	2.68
TPA-AP-TP	379, 401	479	63	382, 405	473	57	192	313	516	−5.42	−2.65	2.77
TP-AP-TPA	381, 400	467	67	384, 404	468	65	189	338	530	−5.41	−2.58	2.83

[a] 1×10^{-5} M in chloroform. [b] Film thickness on the glass: 50 nm.

calculated to be 2.5 times greater than the oscillator strength value of pyrene. Comparing oscillator strength values indicated anthracene to be the primary core and pyrene to be the secondary core in this dual-core structure.[12] The primary and the secondary cores mean the main and the secondary contributors to absorbance and emission of light.

Since anthracene is the primary core of the dual core, substitution of an electron-donating side group into anthracene is expected to yield greater changes of the intrinsic properties of the final compound compared to a substitution into pyrene.

To determine the effects of changing the substitution position of the side group, four types of molecules that introduced *m*-terphenyl, diphenylamine, and triphenylamine moieties as side groups were synthesized: diphenyl-[10-(6-[1,1′;3′,1″]terphenyl-5′-yl-pyren-1-yl)-anthracen-9-yl]-amine (**DPA-AP-TP**), diphenyl-[6-(10-[1,1′;3′,1″]terphenyl-5′-yl-anthracen-9-yl)-pyren-1-yl]-amine (**TP-AP-DPA**), diphenyl-{4-[10-(6-[1,1′;3′,1″]terphenyl-5′-yl-pyren-1-yl)-anthracen-9-yl]-phenyl}-amine (**TPA-AP-TP**) and diphenyl-{4-[6-(10-[1,1′;3′,1″]terphenyl-5′-yl-anthracen-9-yl)-pyren-1-yl]-phenyl}-amine (**TP-AP-TPA**) (see Scheme 1). Diphenylamine, an electron-donating group, was substituted into the anthracene and pyrene cores to make **DPA-AP-TP** and **TP-AP-DPA**, respectively. These molecules were classified as types (A-1) and (A-2), respectively. **TPA-AP-TP** and **TP-AP-TPA** were formed by the substitution of triphenylamine, a side group in which an additional phenyl ring was added to the link between the core and diphenylamine side group in the type (A) form, and were classified as type (B-1) and (B-2), respectively. These synthesized molecules were compared with **TP-AP-TP**, which consists only of phenyl rings that do not include any hetero-atom. The five compounds were synthesized using boronylation and Suzuki aryl–aryl coupling reactions as illustrated in Fig. S1,† and the synthesized materials were characterized by nuclear magnetic resonance spectroscopy, elemental analysis, and fast atom bombardment mass analysis.

To determine the thermal properties of the synthesized molecules, thermal gravimetric analysis (TGA) and differential scanning calorimetry (DSC) were used, with the results summarized in Table 1. All of the synthesized molecules were quite thermally stable, with T_g values of at least 189 °C and decomposition temperature (T_d) values of at least 488 °C. In particular, **TPA-AP-TP** (B-1) and **TP-AP-TPA** (B-2), perhaps due to their increased molecular weights, displayed excellent T_d values of 516 and 530 °C, respectively. Molecules with high T_d values have an advantage in that the morphology of the material is not easily changed by the heat generated during operation of the OLED device.[13]

Ultraviolet-visible (UV-vis) absorption spectra and related data of the synthesized compounds are shown in Fig. 1 and Table 1. To understand the changes in optical properties,

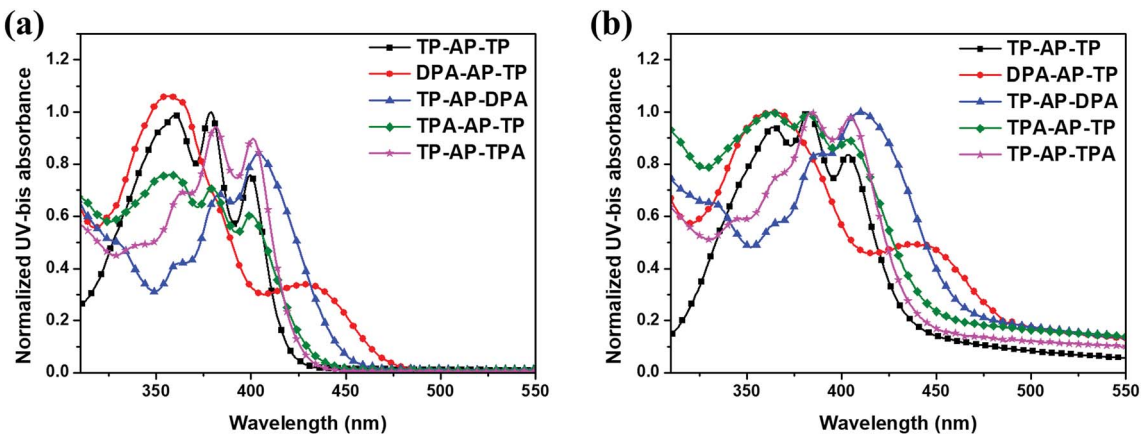

Fig. 1 UV-vis absorption spectra of the synthesized compounds: (a) solution state, (b) film state.

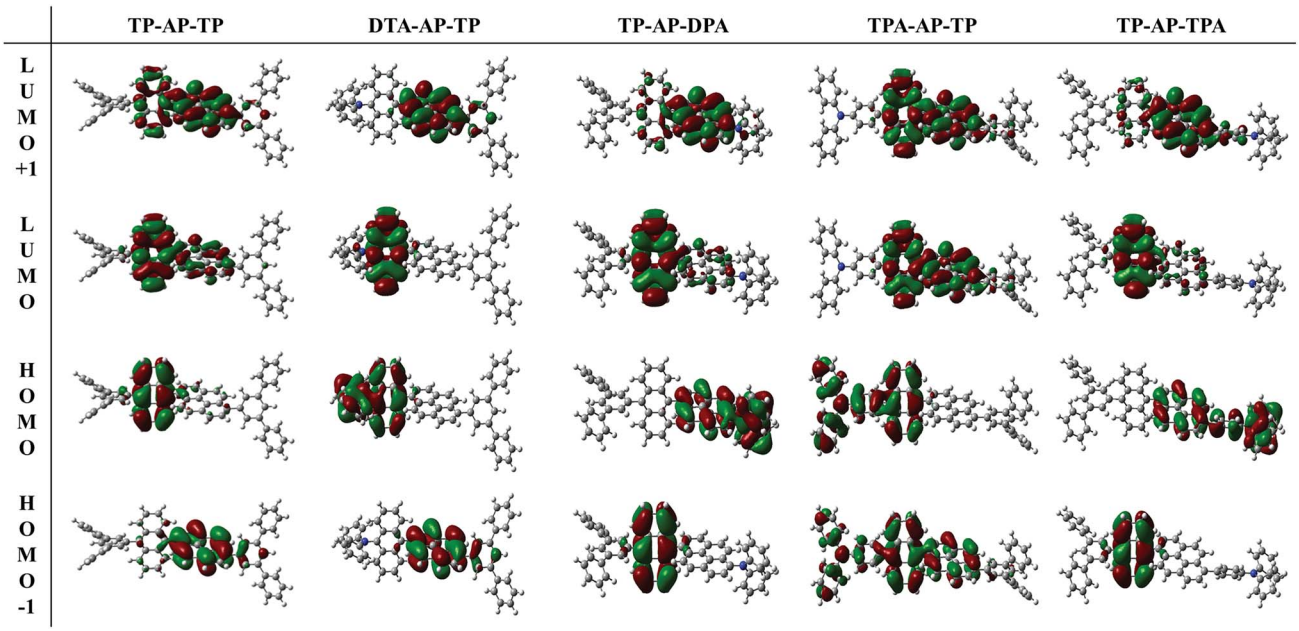

Fig. 2 HOMO−1, HOMO, LUMO and LUMO+1 electronic density distributions of the S_0 states of the compounds calculated at the CAM-B3LYP/6-31G(d) level.

changes in the intramolecular electron density of the molecules were confirmed by density functional theory (DFT) calculations (CAM-B3LYP/6-31G(d) level). Frontier molecular orbitals of the optimized S_0 state molecular structures are shown in Fig. 2. **TP-AP-TP**, with its bulky aromatic side group, showed an absorption wavelength peak of 399 nm in the solution state (Fig. 1a). On the other hand, **DPA-AP-TP** (A-1) and **TP-AP-DPA** (A-2), each containing the electron-donating diphenylamine group, showed absorption wavelength peaks of 428 nm and 404 nm. **TPA-AP-TP** (B-1) and **TP-AP-TPA** (B-2) substituted with a triphenylamine group showed absorption wavelength peaks of 401 nm and 400 nm. The bathochromic (red) shifts of the absorption wavelength peaks of these four compounds relative to that of **TP-AP-TP** may have been due to their having increased conjugation lengths in contrast to **TP-AP-TP**, which only consists of phenyl rings, the type (A) and type (B) molecules substituted with aromatic amine groups were calculated in the HOMO state to display a wide distribution of conjugated electrons, including to the side groups (Fig. 2). The especially large red shift of **DPA-AP-TP** (A-1) (by 29 nm compared to that of **TP-AP-TP**) may have been related to its side group substitution being in the anthracene core, whereas in **TP-AP-DPA** (A-2), with its smaller (5 nm) red shift, the substitution was done into the pyrene core. The particularly small magnitudes of the red shifts displayed by **TPA-AP-TP** (B-1) (by only 2 nm compared to that of **TP-AP-TP**) and **TP-AP-TPA** (B-2) (by only 1 nm), despite the change in their substitution positions, may have been due to the substituted triphenylamine group of these type (B) molecules, with its additional benzene ring, having a relatively reduced electron-donating ability, compared to the diphenylamine group of the type (A) molecules. The UV-vis absorption peak values in the film state (Fig. 1b) were similar to those in the solution state: in the film state, **TP-AP-TP** showed an absorption wavelength peak of 403 nm, **DPA-AP-TP** (A-1) and **TP-AP-DPA** (A-2) showed absorption wavelength peaks of 437 nm and 410 nm, and **TPA-AP-TP** (B-1) and **TP-AP-TPA** (B-2) showed absorption wavelength peak of 405 nm and 404 nm, which were shorter than those of the type (A) molecules.

HOMO, LUMO and band gap levels of the molecules were measured and calculated using the UV-vis absorption data in the film state and ultraviolet photoelectron spectroscopy (Riken-Keiki, AC-2), as presented in Table 1. The HOMO and LUMO levels of **TP-AP-TP** were −6.01 eV and −3.05 eV, yielding a band gap of 2.96 eV. Since both type (A) and type (B) molecules have longer conjugation lengths compared to **TP-AP-TP**, their band gaps were decreased, by 0.26 eV on average: regarding the type (A) molecules, the band gap was 2.51 eV for **DPA-AP-TP** (A-1) (*i.e.*, reduced by 0.45 eV compared to that of **TP-AP-TP**) and was 2.68 eV for **TP-AP-DPA** (A-2) (*i.e.*, reduced by 0.28 eV); regarding the type (B) molecules, the band gap was 2.77 eV for **TPA-AP-TP** (B-1) (*i.e.*, reduced by 0.19 eV compared to that of **TP-AP-TP**) and 2.83 eV for **TP-AP-TPA** (B-2) (*i.e.*, reduced by 0.13 eV). The reduced band gaps of **DPA-AP-TP** (A-1) and of **TPA-AP-TP** (B-1), whose electron-donating groups were substituted into the anthracene core, compared, respectively, to the band gaps of **TP-AP-DPA** (A-2) and **TP-AP-TPA** (B-2), whose side groups were substituted in the pyrene core, occurred despite **DPA-AP-TP** (A-1) and **TP-AP-DPA** (A-2) having the same substituted aromatic amine side group (*i.e.*, diphenylamine) and despite **TPA-AP-TP** (B-1) and **TP-AP-TPA** (B-2) having the same substituted aromatic amine side group (*i.e.*, triphenylamine).

Time dependent (TD)-DFT calculations (TD-CAM-B3LYP/6-31G(d)) of the absorption wavelengths and oscillator strengths (*f*) of the molecules were carried out, and the results of the

Table 2 Absorption frequencies and oscillator strengths calculated with TD-CAM-B3LYP/6-31G(d) for the synthesized compounds

Compounds	λ_{abs} (nm) (oscillator strength (f))	Characteristic transition	Distribution of character[a]	Contribution[b] (%)
TP-AP-TP	352 (0.642)	HOMO → LUMO	A → A + P	75
	319 (0.568)	HOMO−1 → LUMO+1	P → A + P	55
		HOMO−1 → LUMO	P → A + P	24
DPA-AP-TP	381 (0.362)	HOMO → LUMO	A + DPA → A	95
	331 (0.322)	HOMO−2 → LUMO	A + DPA → A	81
TP-AP-DPA	358 (0.910)	HOMO → LUMO+1	P + DPA → P + A	43
		HOMO−1 → LUMO	A → A + P	40
	344 (0.043)	HOMO−1 → LUMO	A → A + P	45
		HOMO → LUMO+1	P + DPA → P + A	37
TPA-AP-TP	355 (0.722)	HOMO → LUMO	A + TPA → A + P	33
		HOMO−1 → LUMO	TPA + A + P → A + P	23
		HOMO → LUMO+1	A + TPA → A + P	18
	319 (0.579)	HOMO−2 → LUMO	TPA + A + P → A + P	30
		HOMO−1 → LUMO+1	TPA + A + P → A + P	27
		HOMO−2 → LUMO+1	TPA + A + P → A + P	21
TP-AP-TPA	353 (0.842)	HOMO−1 → LUMO	A → A	81
	328 (0.643)	HOMO → LUMO+1	P + TPA → P	59
		HOMO−2 → LUMO+1	P + TPA → P	14

[a] A: anthracene, P: pyrene, DPA: diphenylamine, TPA: triphenylamine. [b] When the sum of contributions is less than 100%, the remaining contributions include various small portions of transitions. Only the main process was indicated.

calculations are summarized in Table 2. The wavelength shift tendencies of the UV-vis absorption for the compounds obtained by calculations were similar to the experimental results.

From the determined contribution of the electronic transition in the synthesized compound, **TP-AP-TP** showed an oscillator strength value of 0.642 at a wavelength of 352 nm, and HOMO → LUMO was shown to be the main process characterizing the transition here. The electron density distribution (Fig. 2) showed the anthracene core to be the primary source of this process. The oscillator strength value was 0.568 at 319 nm, and HOMO−1 → LUMO+1 and HOMO−1 → LUMO were found to be the main processes characterizing the electronic transition at this wavelength. The pyrene core was the main source of this process. Comparison of the oscillator strength values at these two wavelengths confirmed the electronic transition in which anthracene participated, rather than that in which the pyrene participated, to be the main factor in the overall process.[12]

Among the type (A) molecules, **DPA-AP-TP** (A-1), in which the electron-donating diphenylamine group was substituted into the anthracene core, showed oscillator strength values of 0.362 and 0.322 at 381 nm and 331 nm, respectively. In these two electronic transition processes, the contribution of the anthracene core was found to be the main factor. On the other hand, **TP-AP-DPA** (A-2), in which the electron-donating group was substituted into the pyrene core, showed an oscillator strength value of 0.910 at 358 nm. Here, the contribution of the electronic transition related to the pyrene core was clearly increased to show the transition process of pyrene.

Similar to type (A) molecules, type (B) molecules also showed an increased electronic transition contribution from each core to which an aromatic amine group was connected. **TPA-AP-TP** (B-1), in which the triphenylamine group was substituted into the anthracene core, showed oscillator strength values of 0.722 and 0.579 at 355 nm and 319 nm, respectively, and anthracene acted as the main core. **TP-AP-TPA** (B-2) showed a high oscillator strength value of 0.842 at 353 nm, with a large contribution of the anthracene core. An oscillator strength value of 0.643 was also shown at 328 nm, and the pyrene core provided the main source of this electronic transition.

While the contribution of the pyrene core to the electronic transition was increased in **TP-AP-TPA** (B-2) showed electronic transition characteristics similar to those of **TP-AP-TP** despite substitution of triphenylamine into the pyrene core. This similarity is due to the electron-donating ability of triphenylamine being smaller than that of diphenylamine and hence the triphenylamine group could not change the contribution of pyrene by much. The computational results are consistent with the experimental results, where, among the four type (A) and type (B) materials, **TP-AP-TPA** (B-2) showed the smallest difference in the band gap compared to that of **TP-AP-TP**.

The direct attachment of an aromatic amine group to the primary anthracene core results in electron donation to this core. This effect is larger for the connection to an anthracene core than that of the connection to a secondary pyrene core. Thus, as was shown from the results of the optical experiments (such as UV-vis absorption and band gaps), the properties of the **DPA-AP-TP** (A-1) and **TPA-AP-TP** (B-1) molecules differed from those of **TP-AP-TP** to a greater extent than did the properties of the **TP-AP-DPA** (A-2) and **TP-AP-TPA** (B-2) molecules.

Photoluminescence (PL) spectra of the synthesized compounds were acquired, and the corresponding data are shown in Fig. 3 and Table 1. **TP-AP-TP** showed a PL maximum (PL_{max}) value at 446 nm in the solution state.

Regarding the type (A) molecules, **DPA-AP-TP** (A-1) showed a PL_{max} at 513 nm, *i.e.*, red shifted by 67 nm compared to that of

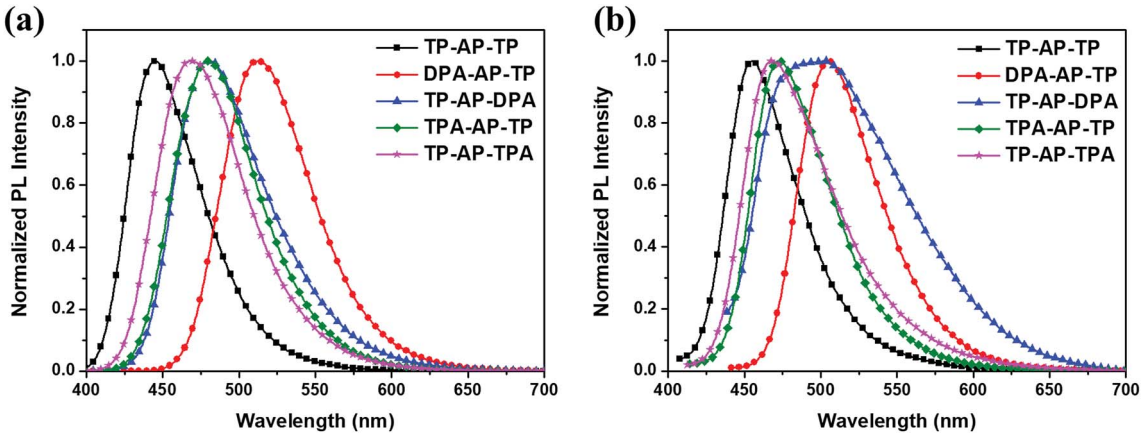

Fig. 3 Normalized PL spectra of the synthesized materials: (a) solution state, (b) film state.

TP-AP-TP, and **TP-AP-DPA** (A-2) showed a PL_{max} at 481 nm, *i.e.*, red shifted by 35 nm. The large red shift of the PL_{max} value of **DPA-AP-TP** (A-1), in which a diphenylamine group was substituted into anthracene, was due to its greatly reduced band gap.[10] On the other hand, type (B) molecules substituted with the triphenylamine group, which has a relatively small electron-donating effect, showed emissions in the shorter wavelength region compared to type (A) molecules: **TPA-AP-TP** (B-1) showed a PL_{max} at 479 nm, *i.e.*, red shifted by 33 nm compared to that of **TP-AP-TP**; and **TP-AP-TPA** (B-2) showed a PL_{max} at 467 nm, *i.e.*, red shifted by 21 nm.

The FWHM values of the PL spectra were also analyzed. In the solution state, **TP-AP-TP** showed a narrow value of 56 nm, whereas the type (A) and type (B) molecules, in which an aromatic amine group was substituted into the core, showed FWHM values increased to 63–67 nm. This increase can be interpreted as a diversification of the electronic transition channels due to a broadened distribution of intramolecular electron density following substitution of an electron donating

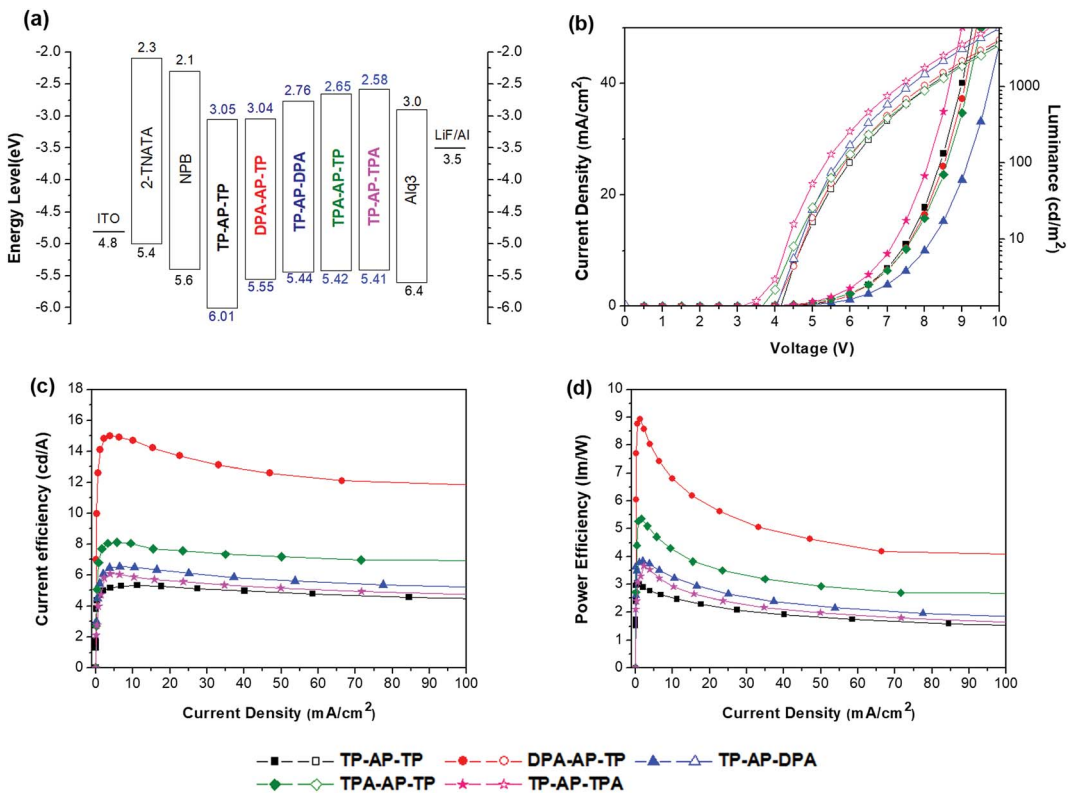

Fig. 4 EL characteristics of devices using the synthesized compounds as EMLs: (a) energy levels of the organic materials, (b) *I*–*V*–*L* curves, (c) current efficiency (CE) *versus* current density, and (d) power efficiency (PE) *versus* current density.

Table 3 Electroluminescence efficiency of the synthesized compounds at 10 mA cm^{-2}: ITO/2-TNATA (60 nm)/NPB (15 nm)/emitting layer (35 nm)/Alq3 (20 nm)/LiF (1 nm)/Al

Compound	Volt (v)	CE (cd A^{-1})	PE (lm W^{-1})	CIE (x,y)	EL (nm)	EL FWHM (nm)
TP-AP-TP	7.19	5.34	2.58	(0.15, 0.13)	456	55
DPA-AP-TP	7.49	13.05	6.83	(0.19, 0.56)	501	57
TP-AP-DPA	6.93	6.50	3.27	(0.24, 0.51)	504	69
TPA-AP-TP	6.56	8.05	4.25	(0.14, 0.24)	473	53
TP-AP-TPA	6.96	5.89	2.96	(0.16, 0.29)	472	57

side group into the core.[14] Increases in the FWHM values of the type (A) and type (B) molecules were also shown in film state. An especially high FWHM value of 106 nm, with two PL_{max} values, at 487 nm and 502 nm, were observed for the film state of the **TP-AP-DPA** (A-2) molecule, in which diphenylamine was substituted into pyrene. This feature was probably caused by a solid-state-specific intermolecular excimer. To clarify whether the emissions at, say, 502 nm is excimer peak corresponding to PL emission from the molecule, excitation spectra were measured along with the UV-vis absorption spectrum (see Fig. S2†). The UV-vis absorption spectrum matched well with the excitation spectra. The excitation spectra monitored at 487 nm and 502 nm were observed to be very similar, indicating that they arose from the same excitation pathway. This finding is consistent with the value at 502 nm resulting from an excimer emission. Also, as shown in Fig. S3,† **TP-AP-DPA** (A-2) displays a dihedral angle between its pyrene and side group of only 68° and has a relatively small side group, and would hence appear to have a reduced ability to prevent intermolecular packing and excimer formation compared to **DPA-AP-TP** (A-1), which, while also having a relatively small side group, displays an increased dihedral angle between its anthracene and side group of 75°. Therefore, in addition to the size of the side group, the dihedral angle by itself may be a factor determining excimer formation. In case of **TP-AP-TPA** (B-2), it did not show excimer emission because of a relatively large side group.

2.2 Electroluminescence properties

Five different non-doped OLED devices (device configuration: ITO/4,4′,4″-tris[2-naphthyl(phenyl)amino]triphenylamine [2-TNATA] 60 nm/*N*,N′-bis(naphthalen-1-yl)-*N*,*N*′-bis(phenyl) benzidine [NPB] 15 nm/synthesized emitting materials 35 nm/ tris(8-hydroxyquinolinato)aluminum [Alq3] 20 nm/LiF 1 nm/Al 200 nm) were prepared using the five synthesized molecules as the respective emitting layers (EMLs), and the EL performances of the devices were measured. 2-TNATA was used as the hole-injection layer, NPB as the hole-transporting layer, and Alq3 as the electron-transporting layer. Emitting materials were applied as a single layer with a non-doped structure.

For each of the five devices, the shape and maximum wavelength of the EL spectrum remained unchanged as the luminance was increased from 500 cd m^{-2} to 3000 cd m^{-2} (see Fig. S4†). All of the devices were confirmed to properly form excitons in the EML and operate stably. The OLED device properties are summarized in Fig. 4 and Table 3.

As was observed for its emission properties, **TP-AP-TP** of the reference material, which only consists of phenyl rings, yielded an EL maximum (EL_{max}) wavelength of 456 nm and blue color coordinates with Commission International de L'Eclairge (CIE) coordinates (x,y) of (0.15, 0.13). Also, it showed a CE of 5.34 cd A^{-1} and power efficiency (PE) of 2.58 lm W^{-1} under a current density of 10 mA cm^{-2}. Compared to **TP-AP-TP**, devices that applied type (A) and type (B) molecules as the EML showed shifting of the emission wavelength to longer wavelengths, as found for PL, but both CE and PE were increased (see Fig. 5). These shifts were caused by the electron-donating aromatic amine moieties.[10]

DPA-AP-TP (A-1) yielded the highest device efficiencies of 13.05 cd $A^{-1}$and 6.83 lm W^{-1}, but an emission with CIEx,y (0.19, 0.56) due to the squeezed band gap. **TP-AP-DPA** (A-2) showed EL efficiencies of 6.50 cd $A^{-1}$and 3.27 lm W^{-1} and a CIEx,y (0.24, 0.51). Also, EL efficiencies of **TPA-AP-TP** (B-1) were 8.05 cd A^{-1} and 4.25 lm W^{-1}, and EL efficiencies of **TP-AP-TPA** (B-2) were 5.89 cd A^{-1} and 2.96 lm W^{-1}. They yielded color coordinate values of CIEx,y (0.14, 0.24) and CIEx,y (0.16, 0.29), respectively. MADN and DPVBi, which are well-known blue reference emitters, showed CE values of 2.86 and 3.92 cd A^{-1}, PE values of 1.48 and 1.61 lm W^{-1}, and EL maximum values of 454 and 465 nm, respectively [see Table S1†]. Comparing to the data of the reference emitters, **TPA-AP-TP** had over two times higher CE and PE values than those of MADN and DPVBi although EL maximum value was red-shifted 7–18 nm compared to MADN and DPVBi.

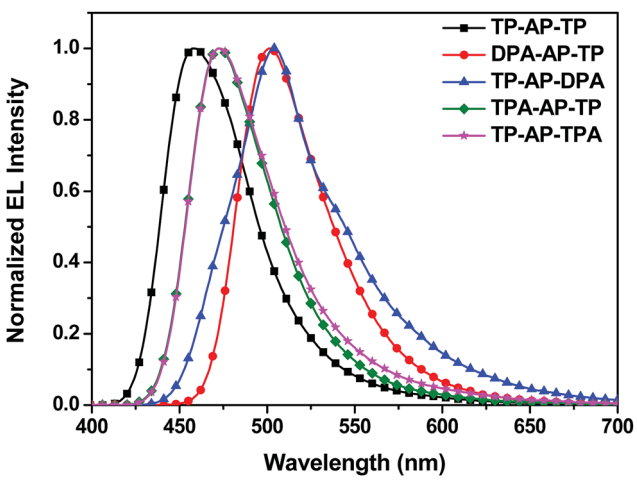

Fig. 5 EL spectra of devices using the synthesized compounds.

Comparing CE and CIE*x*,*y* values of type (A) and type (B) molecules, type (A) molecules substituted with the diphenylamine group showed higher CE values compared to type (B) molecules. However, the EL emission was shifted more to longer wavelengths, and CIE*x*,*y* values were also increased. On the other hand, type (B) molecules, with their triphenylamine group and its reduced electron-donating ability, displayed a relatively small shift of the EL wavelength and were found to have optimized CIE*x*,*y* values for the sky-blue color. The **TPA-AP-TP** (B-1) molecule, with its bulky triphenylamine side group substituted into the primary anthracene core, yielded especially excellent EL efficiencies of 8.05 cd A^{-1} and 4.25 lm W^{-1} as well as a narrow FWHM value of 53 nm. This study verified that in heterocore molecules such as the AP core, one of the two cores functions as the primary core and contributes more to the electronic transition than does the other, *i.e.*, secondary, core—and that the largest changes to the optical and electronic properties of the final heterocore derivatives can be achieved by simply substituting an electron-donating side group into a position on the primary core. Such a methodology could be applied to develop excellent blue light-emitting materials applicable to OLED lighting.

3. Conclusions

This study examined hetero dual-core chromophores in which anthracene and pyrene are connected. The hetero dual-core chromophores included anthracene to be the primary core and pyrene to be the secondary core. We specifically investigated the effects of changing the side group on the performance properties of the final compounds. A nitrogen atom was introduced in order to increase electron donation to the dual core and hence increased device efficiency, and a bulky side group of triphenylamine was introduced to suppress intermolecular interactions. Especially, electron-donating side groups were substituted at different positions of **TP-AP-TP**, a molecule with a hetero dual-core structure, in order to determine whether one of its two cores, and if so which one, contributes more to changes in the optical and electronic properties of the resulting material.

The electron density distribution within the molecule and the part of the molecule contributing to the electronic transition were confirmed to be affected by the substitution of the electronically optimized side group into the core. The **TPA-AP-TP** molecule, whose side group not only displays optimum electron donation to what was determined to be the main core, but also has a proper size, yielded a non-doped OLED device with high efficiency values of 8.05 cd A^{-1} and 4.25 lm W^{-1} as well as a narrow FWHM value of 53 nm. Comparing to the data of the reference emitters, **TPA-AP-TP** had two times higher CE and PE values than those of MADN and DPVBi.

This study verified that the largest changes to the optical and electronic properties of the final heterocore derivatives can be achieved by substituting an electron-donating side group into a position on the primary core.

This systematic methodology can be applied to develop new various other OLED emitters of blue light for OLED lighting based on many multi-core chromophores by introducing various electron-donating moieties to the main core.

4. Experimental section

4.1 General information

The requisite reagents were purchased from Sigma-Aldrich or TCI and were used without further purification, unless otherwise noted. The ^{1}H-NMR spectra were recorded on Bruker Avance 300 spectrometers. The FAB^+-mass and EI^+-spectra were recorded on a JEOL, JMS-AX505WA, HP5890 series II. The optical absorption spectra were obtained by using a Lambda 1050 UV/vis/NIR spectrometer (PerkinElmer). A PerkinElmer luminescence spectrometer LS50 (Xenon flash tube) was used to perform photoluminescence spectroscopy. The glass-transition temperatures (T_g) of the compounds were determined with differential scanning calorimetry (DSC) under a nitrogen atmosphere by using a DSC4000 (PerkinElmer). Samples were heated to 500 °C at a rate of 10 °C min^{-1} and cooled at 10 °C min^{-1} then heated again under the same heating conditions as used in the initial heating process. Degradation temperatures (T_d) were determined with thermo gravimetric analysis (TGA) by using a TGA4000 (PerkinElmer). Samples were heated to 700 °C at a rate of 10 °C min^{-1}. The HOMO energy levels were determined with ultraviolet photoelectron yield spectroscopy (Riken Keiki AC-2). The LUMO energy levels were derived from the HOMO energy levels and the band gaps. All DFT and TD-DFT calculations were performed using the Gaussian09 (ref. 15) program. In each of the EL devices, 4,4′,4″-tris[2-naphthyl(phenyl)amino]triphenylamine (2-TNATA) was used as the hole-injection layer, *N*,*N*′-bis(naphthalen-1-yl)-*N*,5*N*′-bis(phenyl)benzidine (NPB) was used for the hole transporting layer, one of the synthetic materials **TP-AP-TP**, **DPA-AP-TP**, **TP-AP-DPA**, **TPA-AP-TP** and **TP-AP-TPA** were used as the emitting layer (EML), emitting materials were applied as a single layer with a non-doped structure. Tris(8-hydroxyquinolinato)aluminum (Alq3) was used for the electron transporting (ETL), lithium fluoride (LiF) was used for the electron injection layer (EIL), and ITO was used as the anode and aluminum (Al) as the cathode. All organic layers were deposited under 10^{-6} Torr, with a rate of deposition of 1.0 Å s^{-1} to create an emitting area of 4 mm^2. The LiF and aluminum layers were continuously deposited under the same vacuum conditions. The luminance efficiency data for the fabricated EL devices were obtained by using a Keithley 2400 electrometer. Light intensities were obtained with a Minolta CS-1000A. The operational stabilities of the devices were measured under encapsulation in a glove box.

4.1.1 Synthesis of compound [1]. 9-Bromoanthracene (Aldrich, 94%) (10 g, 38.9 mmol) was dissolved in 500 mL of anhydrous THF solution and stirred at −78 °C. Then, *n*-butyllithium solution (Aldrich, 1.6 M in hexane) (29.3 mL, 46.7 mmol) was added. Triethyl borate (Aldrich, 99%) (9.3 mL, 54.5 mmol) was added to the reaction after 30 min. After the reaction was finished, the solution was acidified with 2 N HCl solution and extracted with ethyl acetate and water. The organic layer was dried with anhydrous $MgSO_4$ and filtered. The

solution was evaporated. The residue was redissolved in hexane and added to ethyl acetate (50 mL). The precipitate was filtered and washed with hexane to obtain a beige compound (7.3 g, 85%). ^{1}H-NMR (300 MHz, $CDCl_3$, d): 8.46 (s, 1H), 8.12 (d, 2H), 8.01 (d, 2H), 7.48 (m, 4H), 5.07 (s, 2H).

4.1.2 Synthesis of compound [2]. Bromine (TCI, 98%) (10 mL, 194.7 mmol) in $CHCl_3$ (500 mL) was added to a solution of pyrene (TCI, 97%) (20 g, 98.9 mmol) in $CHCl_3$ (500 mL) over 5 h while stirring. The precipitate was collected after 12 h and resolved by fractional crystallization from xylene (11.8 g, 33%). ^{1}H-NMR (300 MHz, $CDCl_3$, d): 8.46 (d, 2H), 8.27 (d, 2H), 8.12 (d, 2H), 8.06 (d, 2H).

4.1.3 Synthesis of compound [3]. 4-Bromotriphenylamine (Aldrich, 97%) (5 g, 15.4 mmol) was added in 200 mL of anhydrous THF solution and stirred at −78 °C, then *n*-butyllithium solution (Aldrich, 2.0 M in cyclohexane) (7.7 mL) was added. Next, triethyl borate (Aldrich, 99%) (3.93 mL) was added to the reaction mixture after 30 min. After the reaction had finished, HCl 35 wt% solution was added to the reaction mixture after 3 h. The reaction mixture was extracted with diethyl ether and water. The organic layer was dried with anhydrous $MgSO_4$ and filtered. The mixture was evaporated. The product was recrystallized from dichloromethane (CH_2Cl_2) and hexane. (yield 65%). ^{1}H-NMR (300 MHz, $CDCl_3$, 25 °C, TMS): $\delta = 8.77$ (m, 2H), 8.63 (d, 1H), 7.62 (m, 3H), 7.35 (t, 2H), 7.22 ppm (m, 4H).

4.1.4 Synthesis of compound [4]. 1,3,5-Tribromobenzene (Aldrich, 98%) (20 g, 63 mmol), $Pd(PPh_3)_4$ (Aldrich, 99%) (4.36 g, 3.7 mmol) were added to 500 mL of dry THF solution. Then, phenylboronic acid (Aldrich, 95%) (17 g, 140 mmol) and 2 M K_2CO_3 solution (50 mL), which was dissolved in H_2O, was added to the reaction mixture. The reaction mixture was heated to 65 °C for 5 h under nitrogen. After the reaction was finished, diethyl ether and water were extracted. The organic layer was dried with anhydrous $MgSO_4$ and filtered. The solvent was evaporated. The product was isolated by silica gel column chromatography using $CHCl_3$: hexane (1 : 15) eluent to afford a white solid. (Yield 61%) ^{1}H NMR (300 MHz, $CDCl_3$, 25 °C, TMS): $\delta = 7.70$ (s, 3H), 7.60 (d, 4H), 7.44 (t, 4H), 7.36 ppm (t, 2H).

4.1.5 Synthesis of compound [5]. Compound 1 (6.0 g, 19.4 mmol) was dissolved in 400 mL of anhydrous THF solution and stirred at −78 °C. Then, the *n*-butyllithium solution (Aldrich, 2.0 M in cyclohexane) (10 mL) was added. Then, isopropoxy-4,4,5,5-tetramethyl-1,3,2-dioxaborolane (Aldrich, 98%) (6 mL) was added to the reaction mixture. After the reaction was finished, diethyl ether and water were extracted. The organic layer was dried by evaporator. The product was recrystallized from chloroform and methanol. (Yield 86.9%) ^{1}H NMR (300 MHz, $CDCl_3$, 25 °C, TMS): $\delta = 8.03$ (s, 2H), 7.90 (s, 1H), 7.69 (d, 4H), 7.44 (t, 4H), 7.35 (t, 2H), 1.37 ppm (s, 12H).

4.1.6 Synthesis of compound [6]. Compound 2 (9.7 g, 27.0 mmol) and $Pd(PPh_3)_4$ (Aldrich, 99%) (0.62 g, 0.54 mmol) were added to 150 mL of anhydrous toluene solution. Then, compound 1 (4 g, 18.0 mmol), anhydrous ethanol (8 mL), and 2 M K_2CO_3 solution (15 mL) dissolved in H_2O were added to the reaction mixture. The mixture was heated to 65 °C for 5 h under nitrogen. After the reaction was finished, the reaction mixture was extracted with toluene and water. The organic layer was dried with anhydrous $MgSO_4$ and filtered. The solution was evaporated. The product was isolated with silica gel column chromatography by using CH_2Cl_2 : *n*-hexane (1 : 7) as the eluent to afford a beige solid. (3.9 g, 32%). ^{1}H-NMR (300 MHz, $CDCl_3$, d): 8.65 (s, 1H), 8.55 (d, 1H), 8.41 (d, 1H), 8.32 (d, 1H), 8.24 (d, 1H), 8.16 (d, 2H), 8.06 (d, 1H), 7.93 (d, 1H) 7.72 (d, 1H), 7.47 (t, 2H), 7.33 (d, 1H), 7.30 (d, 2H), 7.22 (t, 2H).

4.1.7 Synthesis of compound [7]. Compound 6 (1.0 g, 2.19 mmol) and *N*-bromosuccinimide (Aldrich, 99%) (0.43 g, 2.42 mmol) were added to 30 mL of $CHCl_3$, and acetic acid (5 mL) was added to the reaction mixture. The mixture was refluxed for 2 h. After the reaction was finished, the reaction mixture was extracted with $CHCl_3$ and water. The organic layer was dried with anhydrous $MgSO_4$ and filtered. The solution was evaporated. The residue was re-dissolved in ethanol and added to $CHCl_3$ (50 mL). The precipitate was filtered and washed with ethanol to obtain a yellow compound (1.1 g, 96%). ^{1}H-NMR (300 MHz, $CDCl_3$, d): 8.69 (d, 2H), 8.57 (d, 1H), 5.42 (d, 1H), 8.33 (d, 1H), 8.25 (d, 1H), 8.03 (d, 1H), 7.95 (d, 1H), 7.74 (d, 1H), 7.60 (m, 2H), 7.30 (d, 2H), 7.29 (d, 1H), 7.26 (m, 2H).

4.1.8 Synthesis of TP-AP-TP [8]. Compound 5 (0.8 g, 4.8 mmol), compound 7 (1.0 g, 1.9 mmol), $Pd(OAc)_2$ (Aldrich, 98%) (0.04 g, 0.19 mmol), and $(cyclohexyl)_3P$ (Aldrich) (0.13 g, 0.46 mmol) were added to anhydrous THF (100 mL) solution. Then, tetraethylammonium hydroxide (20 wt%) (10 mL) was added to the reaction mixture. The mixture was heated to 85 °C for 2 h under nitrogen. After the reaction was finished, the reaction mixture was extracted with $CHCl_3$ and water. The organic layer was dried with anhydrous $MgSO_4$ and filtered. The solution was evaporated. The residue was re-dissolved in $CHCl_3$ and added to ethanol. The precipitate was filtered and washed with ethanol. The yellowish powder was purified by using column chromatography with CH_2Cl_2 : *n*-hexane (1 : 7) as the eluent to afford a beige solid (**TP-AP-TP**) (1.0 g, 63%). ^{1}H-NMR (500 MHz, $CDCl_3$, d): 8.43 (d, 1H), 8.40 (d, 1H), 8.22 (d, 1H), 8.21 (d, 1H), 8.11 (d, 2H), 8.08 (s, 1H), 7.97 (m, 3H), 7.89 (m, 4H), 7.79 (m, 9H), 7.50 (m, 9H), 7.40 (m, 8H), 7.21 (t, 2H); ^{13}C-NMR (500 MHz, $CDCl_3$, d): 142.31, 141.99, 141.92, 141.04, 140.87, 140.12, 137.88, 137.39, 135.66, 134.40, 131.28, 131.02, 130.98, 130.72, 130.07, 129.71, 129.19, 129.00, 128.94, 128.92, 128.44, 127.91, 127.84, 127.82, 127.64, 127.42, 127.38, 127.22, 127.19, 125.94, 125.61, 125.39, 125.35, 125.20, 125.14, 125.10, 124.94, 124.74; HRMS (EI, *m*/*z*): $[M]^+$ calcd for $C_{56}H_{42}$, 834.3287; found, 834.3289. Anal. calcd for $C_{56}H_{42}$: C 94.93, H5.07; found: C 94.23, H 5.06%.

4.1.9 Synthesis of compound [9]. Compound 6 (2 g, 4.3 mmol), $Pd(PPh_3)_4$ (Aldrich, 99%) (0.15 g, 0.13 mmol) were added to 50 mL of anhydrous THF solution. Then, compound 5 (2.3 g, 6.4 mmol) and 2 M K_2CO_3 solution (10 mL), which was dissolved in H_2O, was added to the reaction mixture. The reaction mixture was heated to 85 °C for 3 h under nitrogen. After the reaction was finished, diethyl ether and water were extracted. The organic layer was dried with anhydrous $MgSO_4$ and filtered. The solvent was evaporated. The product was isolated by silica gel column chromatography using $CHCl_3$: hexane (1 : 5) eluent to afford a white solid. (Yield 61%) ^{1}H NMR (300 MHz, DMSO, 25 °C, TMS): $\delta = 8.88$ (s, 1H), 8.56 (d,

1H), 8.38 (t, 3H), 8.28 (t, 3H), 8.11 (m, 2H), 8.08 (d, 1H), 7.95 (m, 6H), 7.56 (t, 6H), 7.46 (t, 2H), 7.34 (t, 2H), 7.23 (m, 3H).

4.1.10 Synthesis of compound [10]. Compound 9 (1.0 g, 1.6 mmol) and *N*-bromosuccinimide (Aldrich, 99%) (0.32 g, 1.8 mmol) were added to 30 mL of $CHCl_3$, and acetic acid (3 mL) was added to the reaction mixture. The mixture was refluxed for 3 h. After the reaction was finished, the reaction mixture was extracted with $CHCl_3$ and water. The organic layer was dried with anhydrous $MgSO_4$ and filtered. The solution was evaporated. The residue was re-dissolved in ethanol and added to $CHCl_3$ (50 mL). The precipitate was filtered and washed with ethanol to obtain a yellow compound (yield 76%). ^{1}H-NMR (300 MHz, [D_6] DMSO 25 °C, TMS): 8.65 (d, 2H), 8.55 (d, 1H), 8.37 (t, 3H), 8.25 (d, 1H), 8.09 (m, 2H), 8.02 (d, 1H), 7.94 (m, 6H), 7.77 (m, 2H), 7.56 (t, 4H), 7.47 (m, 4H), 7.29 (d, 2H), 7.16 (d, 1H).

4.1.11 Synthesis of DPA-AP-TP [11]. Compound 10 (1.0 g, 1.4 mmol), diphenylamine (Aldrich, 98%) (0.36 g, 2.1 mmol), $Pd_2(dba)_3$ (Aldrich, 97%) (0.07 g, 0.07 mmol), sodium tetra butoxide (Aldrich, 97%) (0.67 g, 7.0 mmol) were added to 100 mL of dry toluene solution. The reaction mixture was heated to 100 °C for 10 h under nitrogen. After the reaction was finished, chloroform and water were extracted. The organic layer was dried with anhydrous $MgSO_4$ and filtered. The solvent was evaporated. The product was isolated by silica gel column chromatography using $CHCl_3$: hexane (1 : 5) eluent to afford a white solid (yield 68%). ^{1}H-NMR (300 MHz, [D_8] THF 25 °C, TMS): 8.46 (d, 1H), 8.43 (d, 1H), 8.29 (m, 4H), 8.19 (d, 1H), 8.10 (d, 1H), 8.06 (m, 1H), 7.94 (m, 3H), 7.86 (d, 4H), 7.49 (t, 4H), 7.40 (m, 7H), 7.22 (m, 10H), 6.91 (m, 2H). EI$^+$-mass: 773, HRMS (EI, *m*/*z*): [M^+] calcd for $C_{60}H_{39}N_1$, 773.3082; found, 773.3080. Anal. calcd for $C_{60}H_{39}N_1$: C 93.11, H 5.08, N 1.81; found: C 92.62, H 5.07, N 1.80%.

4.1.12 Synthesis of TPA-AP-TP [12]. Compound 10 (1.0 g, 1.4 mmol), $Pd(PPh_3)_4$ (Aldrich, 99%) (0.08 g, 0.07 mmol) were added to 100 mL of anhydrous toluene solution. Then, compound 3 (0.61 g, 2.1 mmol) and 2 M K_2CO_3 solution (8 mL), which was dissolved in H_2O, was added to the reaction mixture. The reaction mixture was heated to 110 °C for 5 h under nitrogen. After the reaction was finished, chloroform and water were extracted. The organic layer was dried with anhydrous $MgSO_4$ and filtered. The solvent was evaporated. The product was isolated by silica gel column chromatography using $CHCl_3$: hexane (1 : 4) eluent to afford a white solid. (Yield 76%) ^{1}H NMR (300 MHz, [D_8] THF 25 °C, TMS): δ = 8.46 (d, 1H), 8.42 (d, 1H), 8.29 (d, 2H), 8.18 (d, 1H), 8.07 (m, 2H), 7.86 (m, 9H), 7.49 (t, 5H), 7.37 (m, 18H), 7.20 (t, 2H), 7.08 (t, 2H). EI$^+$-mass: 849, HRMS (EI, *m*/*z*): [M^+] calcd for $C_{66}H_{43}N_1$, 849.3395; found, 849.3393. Anal. calcd for $C_{66}H_{43}N_1$: C 93.25, H 5.10, N 1.65; found: C 93.15, H 4.99, N 1.64%.

4.1.13 Synthesis of compound [13]. 9.10-Dibromoanthracene (2.0 g, 5.9 mmol), $Pd(PPh_3)_4$ (Aldrich, 99%) (0.2 g, 0.17 mmol) were added to 100 mL of anhydrous THF solution. Then, compound 5 (2.1 g, 5.9 mmol) and 2 M K_2CO_3 solution (5 mL), which was dissolved in H_2O, was added to the reaction mixture. The reaction mixture was heated to 65 °C for 4 h under nitrogen. After the reaction was finished, chloroform and water were extracted. The organic layer was dried with anhydrous $MgSO_4$ and filtered. The solvent was evaporated. The product was isolated by silica gel column chromatography using $CHCl_3$: hexane (1 : 9) eluent to afford a white solid. (Yield 48%) ^{1}H NMR (300 MHz, $CDCl_3$ 25 °C, TMS): δ = 8.46 (d, 1H), 8.64 (d, 2H), 8.03 (s, 1H), 7.82 (d, 2H), 7.72 (d,4H), 7.65 (m, 2H), 7.60 (m, 2H), 7.42 (m, 8H).

4.1.14 Synthesis of compound [14]. Compound 13 (2 g, 4.1 mmol) was added in 100 mL of anhydrous THF solution and stirred at −78 °C, then *n*-butyllithium solution (Aldrich, 2.0 M in cyclohexane) (2.1 mL) was added. Next, triethyl borate (Aldrich, 99%) (1.5 mL) was added to the reaction mixture after 30 min. After the reaction had finished, HCl 35wt% solution was added to the reaction mixture after 3 h. The reaction mixture was extracted with diethyl ether and water. The organic layer was dried with anhydrous $MgSO_4$ and filtered. The mixture was evaporated. The product was recrystallized from dichloromethane (CH_2Cl_2) and hexane. (Yield 65%). ^{1}H NMR (300 MHz, $CDCl_3$, 25 °C, TMS): δ = 8.18 (d, 2H), 8.01 (s, 1H), 7.85 (d, 2H), 7.72 (d, 4H), 7.64 (s, 2H), 7.48 (m, 6H), 7.36 (m, 4H), 5.17 (s, 2H).

4.1.15 Synthesis of compound [15]. Compound 14 (2.0 g, 4.4 mmol), $Pd(PPh_3)_4$ (Aldrich, 99%) (0.2 g, 0.17 mmol) were added to 200 mL of anhydrous toluene solution. Then, compound 2 (3.2 g, 8.8 mmol) and 2 M K_2CO_3 solution (10 mL), which was dissolved in H_2O, was added to the reaction mixture. The reaction mixture was heated to 85 °C for 3 h under nitrogen. After the reaction was finished, chloroform and water were extracted. The organic layer was dried with anhydrous $MgSO_4$ and filtered. The solvent was evaporated. The product was isolated by silica gel column chromatography using $CHCl_3$: hexane (1 : 5) eluent to afford a white solid. (Yield 42%) ^{1}H NMR (300 MHz, $CDCl_3$ 25 °C, TMS): δ = 8.60 (d, 1H), 8.48 (d, 1H), 8.38 (d, 1H), 8.26 (d, 1H), 8.15 (d, 1H), 8.07 (s, 1H), 7.95 (m, 3H), 7.88 (s, 1H), 7.83 (m, 6H), 7.52 (m, 5H), 7.43 (m, 6H), 7.22 (t, 2H).

4.1.16 Synthesis of TP-AP-DPA [16]. Compound 15 (1.0 g, 1.4 mmol), diphenylamine (Aldrich, 98%) (0.36 g, 2.1 mmol), $Pd_2(dba)_3$ (Aldrich, 97%) (0.07 g, 0.07 mmol), sodium tetra butoxide (Aldrich, 97%) were added to 100 mL of anhydrous toluene solution. The reaction mixture was heated to 100 °C for 10 h under nitrogen. After the reaction was finished, chloroform and water were extracted. The organic layer was dried with anhydrous $MgSO_4$ and filtered. The solvent was evaporated. The product was isolated by silica gel column chromatography using $CHCl_3$: hexane (1 : 4) eluent to afford a white solid (yield 58%). ^{1}H-NMR (300 MHz, [D_8] THF 25 °C, TMS): 8.42 (d, 1H), 8.30 (d, 1H), 8.19 (m, 3H), 8.09 (d, 1H), 7.90 (m, 10H), 7.49 (m, 4H), 7.37 (m, 7H), 7.24 (t, 6H), 7.11 (d, 4H), 6.97 (t, 2H). EI$^+$-mass: 773, HRMS (EI, *m*/*z*): [M^+] calcd for $C_{60}H_{39}N_1$, 773.3082; found, 773.3092. Anal. calcd for $C_{60}H_{39}N_1$: C 93.11, H 5.08, N 1.81; found: C 92.78, H 5.14, N 1.83%.

4.1.17 Synthesis of TP-AP-TPA [17]. Compound 15 (1.0 g, 1.4 mmol), $Pd(PPh_3)_4$ (Aldrich, 99%) (0.08 g, 0.07 mmol) were added to 100 mL of anhydrous toluene solution. Then, compound 3 (0.8 g, 2.8 mmol) and 2 M K_2CO_3 solution (5 mL), which was dissolved in H_2O, was added to the reaction mixture. The reaction mixture was heated to 100 °C for 4 h under nitrogen. After the reaction was finished, chloroform and water

were extracted. The organic layer was dried with anhydrous $MgSO_4$ and filtered. The solvent was evaporated. The product was isolated by silica gel column chromatography using $CHCl_3$: hexane (1 : 4) eluent to afford a white solid. (Yield 62%) ^{1}H NMR (300 MHz, [D_8] THF 25 °C, TMS): δ = 8.42 (d, 1H), 8.30 (d, 1H), 8.18 (m, 3H), 8.13 (d, 1H), 7.93 (m, 10H), 7.51 (m, 4H), 7.37 (m, 7H), 7.22 (t, 6H), 7.11 (d, 4H), 6.95 (t, 2H). EI$^+$-mass: 849, HRMS (EI, *m*/*z*): [M^+] calcd for $C_{66}H_{43}N_1$, 849.3395; found, 849.3390. Anal. calcd for $C_{66}H_{43}N_1$: C 93.25, H 5.10, N 1.65; found: C 92.90, H 4.97, N 1.70%.

Conflicts of interest

There are no conflicts to declare.

Acknowledgements

This research was supported by National R&D Program through the National Research Foundation of Korea (NRF) funded by the Ministry of Science & ICT (No. 2017M3A7B4041699). This research was supported by Basic Science Research Program through the National Research Foundation of Korea (NRF) funded by the Ministry of Education (No. 2017R1D1A1A09082138).

Notes and references

1 (*a*) C. W. Tang and S. A. Van Slyke, *Appl. Phys. Lett.*, 1987, **51**, 913; (*b*) Y. R. Sun, N. Giebink, C. Kanno, B. Ma, M. E. Thompson and S. R. Forrest, *Nature*, 2006, **440**, 908; (*c*) M. F. Wu, S. J. Yeh, C. T. Chen, H. Murayama, T. Tsuboi, W. S. Li, I. Chao, S. W. Liu and J. K. Wang, *Adv. Funct. Mater.*, 2007, **17**, 1887; (*d*) Z. Zhao, C. Deng, S. Chen, J. W. Y. Lam, W. Qin, P. Lu, Z. Wang, H. S. Kwok, Y. Ma, H. Qiu and B. Z. Tang, *Chem. Commun.*, 2011, **47**, 8847; (*e*) H. Wu, G. Zhou, J. Zou, C. L. Ho, W. Y. Wong, W. Yang, J. Peng and Y. Cao, *Adv. Mater.*, 2009, **21**, 4181; (*f*) M. C. Gather, A. Kohnen, A. Falcou, H. Becker and K. Meerholz, *Adv. Funct. Mater.*, 2007, **17**, 191; (*g*) J. Huang, X. Wang, A. J. deMello, J. C. deMello and D. D. C. Bradley, *J. Mater. Chem.*, 2007, **17**, 3551; (*h*) B. Chen, J. Ding, L. Wang, X. Jing and F. Wang, *Chem. Commun.*, 2012, **48**, 8970; (*i*) Z. Shen, P. E. Burrows, V. Bulović, S. R. Forrest and M. E. Thompson, *Science*, 1997, **276**, 2009; (*j*) S. R. Forrest, *Org. Electron.*, 2003, **4**, 45; (*k*) A. R. Duggal, J. J. Shiang, C. M. Heller and D. F. Foust, *Appl. Phys. Lett.*, 2002, **80**, 3470; (*l*) B. W. D'Andrade and S. R. Forrest, *Adv. Mater.*, 2004, **16**, 1585; (*m*) M. Yu, S. Wang, S. Shao, J. Ding, L. Wang, X. Jing and F. Wang, *J. Mater. Chem. C*, 2015, **3**, 861; (*n*) L. Zhao, S. Wang, S. Shao, J. Ding, L. Wang, X. Jing and F. Wang, *J. Mater. Chem. C*, 2015, **3**, 8859; (*o*) S. Kim, B. Kim, J. Lee, H. Shin, Y.-I. Park and J. Park, *Mater. Sci. Eng., R*, 2016, **99**, 1; (*p*) J. T. Smith, B. A. Katchman, D. E. Kullman, U. Obahiagbon, Y.-K. Lee, B. P. O'Brien, G. B. Raupp, K. S. Anderson and J. B. Christen, *J. Disp. Technol.*, 2016, **12**, 273; (*q*) B. A. Katchman, J. T. Smith, U. Obahiagbon, S. Kesiraju, Y.-K. Lee, B. O'Brien, K. Kaftanoglu, J. B. Christen and K. S. Anderson, *Sci. Rep.*, 2016, **6**, 29057; (*r*) J. Ynag, J. Huang, Q. Li and Z. Li, *J. Mater. Chem. C*, 2016, **4**, 2663.

2 (*a*) J. H. Jou, C. P. Wang, M. H. Wu, H. W. Lin, H. C. Pan and B. H. Liu, *J. Mater. Chem.*, 2010, **20**, 6626; (*b*) S. Krotkus, D. Kasemann, S. Lenk, K. Leo and S. Reineke, *Light: Sci. Appl.*, 2016, **5**, e16121; (*c*) E. Angioni, M. Chapran, K. Ivaniuk, N. Kostiv, V. Cherpak, P. Stakhira, A. Lazauskas, S. Tamulevičius, D. Volyniuk, N. J. Findlay, T. Tuttle, J. V. Grazulevicius and P. J. Skabara, *J. Mater. Chem. C*, 2016, **4**, 3851; (*d*) H.-J. Kim, M.-H. Shin, H.-G. Hong, B.-S. Song, S.-K. Kim, W.-H. Koo, J.-G. Yoon, S.-Y. Yoon and Y.-J. Kim, *J. Disp. Technol.*, 2016, **12**, 526; (*e*) Y. Chen, J. Wang, Z. Zhong, Z. Jiang, C. Song, Z. Hu, J. Peng, J. Wang and Y. Cao, *Org. Electron.*, 2016, **37**, 458.

3 (*a*) Y. L. Chang, Y. Song, Z. Wang, M. G. Helander, J. Qiu, L. Chai, Z. Liu, G. D. Scholes and Z. Lu, *Adv. Funct. Mater.*, 2013, **23**, 705; (*b*) S. Reineke, F. Lindner, G. Schwartz, N. Seidler, K. Walzer, B. Lüssem and K. Leo, *Nature*, 2009, **459**, 234; (*c*) M. Thomschke, S. Reineke, B. Lüssem and K. Leo, *Nano Lett.*, 2012, **12**, 424; (*d*) L. Zhou, X. Li, X. Li, J. Feng, S. Song and H. Zhang, *J. Phys. Chem. C*, 2010, **114**, 21723; (*e*) H. P. Lin, F. Zhou, J. Li, X. W. Zhang, L. Zhang, X. Y. Jiang, Z. L. Zhang and J. H. Zhang, *J. Phys. Chem. C*, 2011, **115**, 24341; (*f*) S. A. Wang, W. Y. Hung, Y. H. Chen and K. T. Wong, *Org. Electron.*, 2012, **13**, 1576; (*g*) Z. Wu, J. Luo, N. Sun, L. Zhu, H. Sun, L. Yu, D. Yang, X. Qiao, J. Chen, C. Yang and D. Ma, *Adv. Funct. Mater.*, 2016, **26**, 3306.

4 (*a*) X. Yang, H. Huang, B. Pan, M. P. Aldred, S. Zhuang, L. Wang, J. Chen and D. Ma, *J. Phys. Chem. C*, 2012, **116**, 15041; (*b*) L. Duan, D. Zhang, K. Wu, X. Huang, L. Wang and Y. Qiu, *Adv. Funct. Mater.*, 2011, **21**, 3540; (*c*) S. M. Shen, Y. C. Tsai and J. H. Jou, *ACS Appl. Mater. Interfaces*, 2011, **3**, 3134; (*d*) X. Yang, Y. Zhao, X. Zhang, R. Li, J. Dang, Y. Li, G. Zhou, Z. Wu, D. Ma, W. Y. Wong, X. Zhao, A. Ren, L. Wang and X. Hou, *J. Mater. Chem.*, 2012, **22**, 7136; (*e*) R. Springer, B. Y. Kang, R. Lampande, D. H. Ahn, S. Lenk, S. Reineke and J. H. Kwon, *Opt. Express*, 2016, **24**, 28131; (*f*) M. Du, Y. Feng, D. Zhu, T. Peng, Y. Liu, Y. Wang and M. R. Bryce, *Adv. Mater.*, 2016, **28**, 5963.

5 (*a*) N. C. Giebink, B. W. D'Andrade, M. S. Weaver, P. B. Mackenzie, J. J. Brown, M. E. Thompson and S. R. Forrest, *J. Appl. Phys.*, 2008, **103**, 44509; (*b*) I. R. de Moraes, S. Scholz, B. Lussem and K. Leo, *Org. Electron.*, 2011, **12**, 341; (*c*) H. Shin, H. Jung, B. Kim, J. Lee, J. Moon, J. Kim and J. Park, *J. Mater. Chem. C*, 2016, **4**, 3833; (*d*) S. Lee, B. Kim, H. Jung, H. Shin, H. Lee, J. Lee and J. Park, *Dyes Pigm.*, 2016, **136**, 255.

6 (*a*) S.-H. Lin, F.-I. Wu and R.-S. Liu, *Chem. Commun.*, 2009, 6961; (*b*) K. Danel, T.-H. Huang, J. T. Lin, Y.-T. Tao and C.-H. Chuen, *Chem. Mater.*, 2002, **14**, 3860; (*c*) C.-H. Chien, C.-K. Chen, F.-M. Hsu, C.-F. Shu, P.-T. Chou and C.-H. Lai, *Adv. Funct. Mater.*, 2009, **19**, 560; (*d*) C. J. Zheng, W. M. Zhao, Z. Q. Wang, D. Huang, J. Ye, X. M. Ou, X. H. Zhang, C. S. Lee and S. T. Lee, *J. Mater. Chem.*, 2010,

20, 1560; (*e*) C. H. Wu, C. H. Chien, F. M. Hsu, P. I Shih and C. F. Shu, *J. Mater. Chem.*, 2009, **19**, 1464; (*f*) C. J. Kuo, T. Y. Li, C. C. Lien, C. H. Liu, F. I. Wu and M. J. Huang, *J. Mater. Chem.*, 2009, **19**, 1865; (*g*) S. K. Kim, B. Yang, Y. Ma, J. H. Lee and J. Park, *J. Mater. Chem.*, 2008, **18**, 3376; (*h*) H. Shin, H. Kang, B. Kim, Y. Park, Y. J. Yu and J. Park, *Bull. Korean Chem. Soc.*, 2014, **35**, 3041; (*i*) Z. Li, Y. Sun, H. Li, J. Ren, C. Si, X. Lv, J. Yu, H. Wang, F. Shi and Y. Hao, *Synth. Met.*, 2016, **217**, 102; (*j*) X. Wei, L. Bu, X. Li, H. Ågren and Y. Xie, *Dyes Pigm.*, 2017, **136**, 480; (*k*) J. Y. Song, S. N. Park, S. J. Lee, Y. K. Kim and S. S. Yoon, *Dyes Pigm.*, 2015, **114**, 40.

7 (*a*) S. L. Lai, Q. X. Tong, M. Y. Chan, T. W. Ng, M. F. Lo, S. T. Lee and C. S. Lee, *J. Mater. Chem.*, 2011, **21**, 1206; (*b*) T. M. Figueira-Duarte, P. G. D. Rosso, R. Trattnig, S. Sax, E. J. W. List and K. Mullen, *Adv. Mater.*, 2010, **22**, 990; (*c*) K.-C. Wu, P.-J. Ku, C.-S. Lin, H.-T. Shih, F.-I. Wu, M.-J. Huang, J.-J. Lin, I.-C. Chen and C.-H. Cheng, *Adv. Funct. Mater.*, 2008, **18**, 67; (*d*) M. Y. Lo, C. Zhen, M. Lauters, G. E. Jabbour and A. Sellinger, *J. Am. Chem. Soc.*, 2007, **129**, 5808; (*e*) K. R. Justin Thomas, N. Kapoor, M. N. K. Prasad Bolisetty, J.-H. Jou, Y.-L. Chen and Y.-C. Jou, *J. Org. Chem.*, 2012, **77**, 3921; (*f*) A. Islam, Q. Wang, L. Zhang, T. Lei, L. Hong, R. Yang, Z. Liu, R. Peng, L.-S. Liao and Z. Ge, *Dyes Pigm.*, 2017, **142**, 499; (*g*) D. Karthik, K. R. J. Thomas, J.-H. Jou, S. Kumar, Y.-L. Chen and Y.-C. Jou, *RSC Adv.*, 2015, **5**, 8727.

8 (*a*) E. J. W. List, R. Guentner, P. Scanducci de Freitas and U. Scherf, *Adv. Mater.*, 2002, **14**, 374; (*b*) M. S. Gong, H. S. Lee and Y. M. Jeon, *J. Mater. Chem.*, 2010, **20**, 10735; (*c*) Y. M. Jeon, J. Y. Lee, J. W. Kim, C. W. Lee and M. S. Gong, *Org. Electron.*, 2010, **11**, 1844; (*d*) S. O. Jeon, Y. M. Jeon, J. W. Kim, C. W. Lee and M. S. Gong, *Org. Electron.*, 2008, **9**, 522; (*e*) K.-T. Wong, R.-T. Chen, F.-C. Fang, C.-C. Wu and Y.-T. Lin, *Org. Lett.*, 2005, **7**, 1979; (*f*) S. S. Reddy, V. G. Sree, K. Gunasekar, W. Cho, Y.-S. Gal, M. Song, J.-W. Kang and S.-H. Jin, *Adv. Opt. Mater.*, 2016, **4**, 1236; (*g*) S. S. Reddy, V. G. Sree, W. Cho and S.-H. Jin, *Chem.–Asian J.*, 2016, **11**, 3275.

9 (*a*) L. Wang, Z. Y. Wu, W. Y. Wong, K. W. Cheah, H. Huang and C. H. Chen, *Org. Electron.*, 2011, **12**, 595; (*b*) J. K. Park, K. H. Lee, S. Kang, J. Y. Lee, J. S. Park, J. H. Seo, Y. K. Kim and S. S. Yoon, *Org. Electron.*, 2010, **11**, 905; (*c*) J. Y. Hu, Y. J. Pu, F. Satoh, S. Kawata, H. Katagiri, H. Sasabe and J. Kido, *Adv. Funct. Mater.*, 2014, **24**, 2064; (*d*) C. L. Wu, C. H. Chang, Y. T. Chang, C. T. Chen, C. T. Chen and C. J. Su, *J. Mater. Chem. C*, 2014, **2**, 7188.

10 (*a*) D. Bailey and V. E. Williams, *Chem. Commun.*, 2005, 2569; (*b*) Y. Zhang, G. Cheng, Y. Zhao, J. Y. Hou, S. Y. Liu, S. Tang and Y. G. Ma, *Appl. Phys. Lett.*, 2005, **87**, 241112; (*c*) S. Tang, M. Liu, P. Lu, G. Cheng, M. Zeng, Z. Q. Xie, H. Xu, H. P. Wang, B. Yang, Y. G. Ma and D. H. Yan, *Org. Electron.*, 2008, **9**, 241; (*d*) C.-C. Wu, Y.-T. Lin, K.-T. Wong, R.-T. Chen and Y.-Y. Chien, *Adv. Mater.*, 2004, **16**, 61; (*e*) J. H. Jou, M. H. Wu, C. P. Wang, Y. S. Chiu, P. H. Chiang, H. C. Hu and R. Y. Wang, *Org. Electron.*, 2007, **8**, 735; (*f*) S. Tang, W. J. Li, F. Z. Shen, D. D. Liu, B. Yang and Y. G. Ma, *J. Mater. Chem.*, 2012, **22**, 4401; (*g*) S. Tao, Y. l. Jiang, S. L. Lai, M. K. Fung, Y. C. Zhou, X. H. Zhang, W. M. Zhao and C. S. Lee, *Org. Electron.*, 2011, **12**, 358.

11 B. Kim, Y.-I. Park, J. Lee, D. Yokoyama, J. H. Lee, J. Kido and J. Park, *J. Mater. Chem. C*, 2013, **1**, 432.

12 (*a*) H. Lee, B. Kim, S. Kim, J. Kim, J. Lee, H. G. Shin, J. H. Lee and J. Park, *J. Mater. Chem. C*, 2014, **2**, 4737; (*b*) K. Sumi, Y. Niko, K. Tokumaruz and G. Konishi, *Chem. Commun.*, 2013, **49**, 3893; (*c*) Z. Gao, Z. Wang, T. Shan, Y. Liu, F. Shen, Y. Pan, H. Zhang, X. He, P. Lu, B. Yang and Y. Ma, *Org. Electron.*, 2014, **15**, 2667; (*d*) Q. Zhang, H. Kuwabara, W. J. Potscavage Jr, S. Huang, Y. Hatae, T. Shibata and C. Adachi, *J. Am. Chem. Soc.*, 2014, **136**, 18070.

13 (*a*) Y. Park, B. Kim, C. Lee, A. Hyun, S. Jang, J. H. Lee, Y. S. Gal, T. H. Kim, K. S. Kim and J. Park, *J. Phys. Chem. C*, 2011, **115**, 4843; (*b*) S. Ye, J. Chen, C. Di, Y. Liu, K. Lu, W. Wu, C. Du, Y. Liu, Z. Shuai and G. Yu, *J. Mater. Chem.*, 2010, **20**, 3186.

14 Y. Park, J. H. Lee, D. H. Jung, S. H. Liu, Y. H. Lin, L. Y. Chen, C. C. Wu and J. Park, *J. Mater. Chem.*, 2010, **20**, 5930.

15 M. J. Frisch, G. W. Trucks, H. B. Schlegel, G. E. Scuseria, M. A. Robb, J. R. Cheeseman, G. Scalmani, V. Barone, B. Mennucci, G. A. Petersson, H. Nakatsuji, M. Caricato, X. Li, H. P. Hratchian, A. F. Izmaylov, J. Bloino, G. Zheng, J. L. Sonnenberg, M. Hada, M. Ehara, K. Toyota, R. Fukuda, M. I. J. Hasegawa, T. Nakajima, Y. Honda, O. Kitao, H. Nakai, T. Vreven, J. A. Montgomery Jr, J. E. Peralta, F. Ogliaro, M. Bearpark, J. J. Heyd, E. Brothers, K. N. Kudin, V. N. Staroverov, R. Kobayashi, J. Normand, K. Raghavachari, A. Rendell, J. C. Burant, S. S. Iyengar, J. Tomasi, M. Cossi, N. Rega, J. M. Millam, M. Klene, J. E. Knox, J. B. Cross, V. Bakken, C. Adamo, J. Jaramillo, R. Gomperts, R. E. Stratmann, O. Yazyev, A. J. Austin, R. Cammi, C. Pomelli, J. W. Ochterski, R. L. Martin, K. Morokuma, V. G. Zakrzewski, G. A. Voth, P. Salvador, J. J. Dannenberg, S. Dapprich, A. D. Daniels, Ö. Farkas, J. B. Foresman, J. V. Ortiz, J. Cioslowski and D. J. Fox, *Gaussian 09, Revision D. 01*, Gaussian, Inc., Wallingford, CT, 2009.